

Figure S1, related to Figure 1. Effect of fatty acids on cell death. (A) Representative images (from one of three independent biological replicates) showing the suppression of erastin (10 μM)-induced cell death by oleic acid (OA, 250 μM). (B) Quantification of cell viability using the metabolic dye PrestoBlue in HT-1080^N cells following 72 h treatment with erastin ± the vehicle control (ethanol, EtOH), OA or palmitoleic acid (POA). Data represent mean ± SD from two biological replicates and are normalized to the EtOH condition (set to 100%). (C) Cell death over 120 h for 261 bioactive compounds ± OA (125 μM). The lethality of each compound is summarized as the AUC of lethal fraction scores over 120 h (i.e. AUC^{LF}). Each gray dot indicates one compound. Results for each compound were averaged across three independent biological replicates. (D) Cell death in cells treated with oleic acid free fatty acid (OA) or OA conjugated to albumin (BSA-OA), both at 125 μM. Each individual datapoint represents an independent biological replicates.

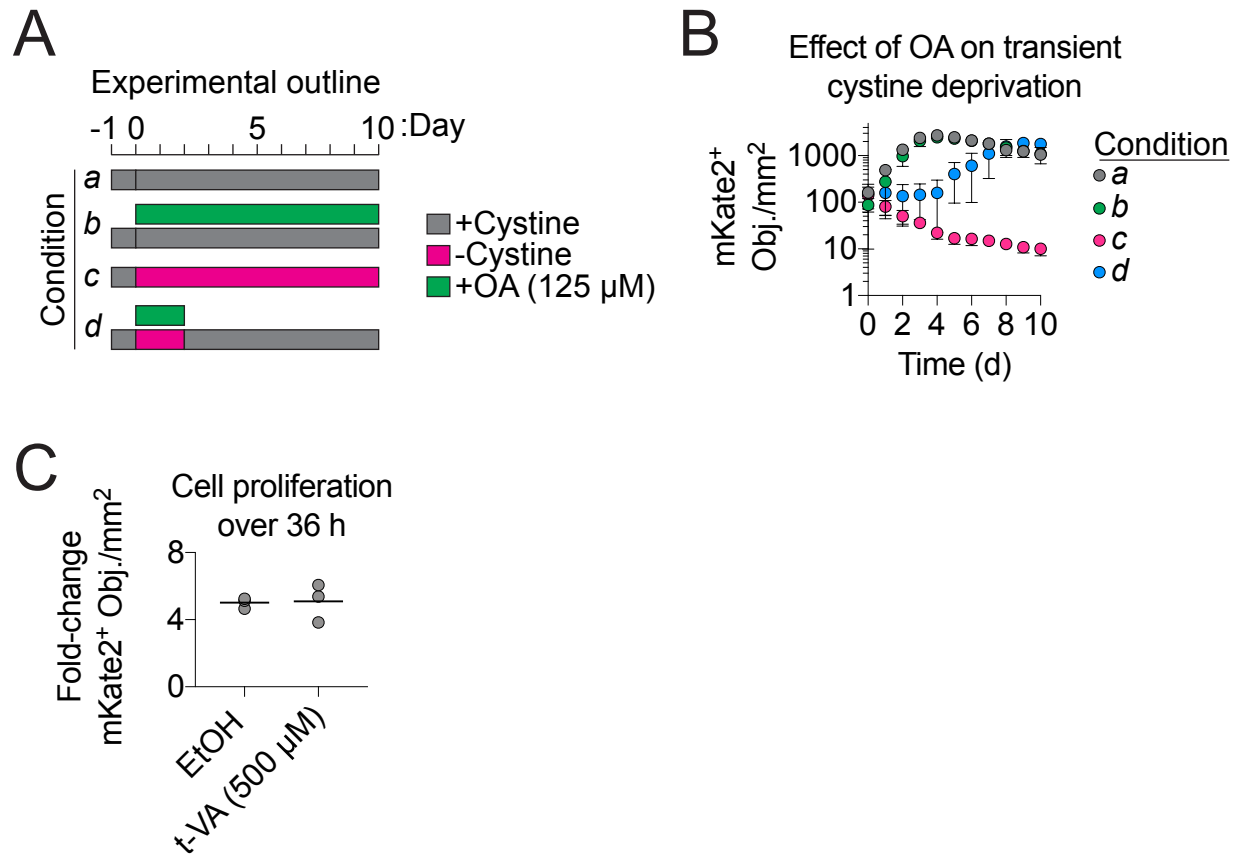


Figure S2, related to Figure 2. MUFAs promote cell viability and do not inhibit cell proliferation. (A) Outline of four treatment conditions (*a-d*) to examine the effects of transient (2 day) cystine deprivation on cell proliferation. OA: oleic acid. (B) HT-1080^N live cell counts (mKate2⁺ objects/mm²) over time in response to the treatment conditions *a-d* explained in (A). Condition labels (*a-d*) correspond to those in (A). Data are mean \pm SD from three independent biological replicates. (C) Fold-change in HT-1080^N live cell counts over 36 h, normalized to the start of the experiment. t-VA: trans-vaccenic acid. Each datapoint represents an independent biological replicate. Mean values are indicated by a black bar.

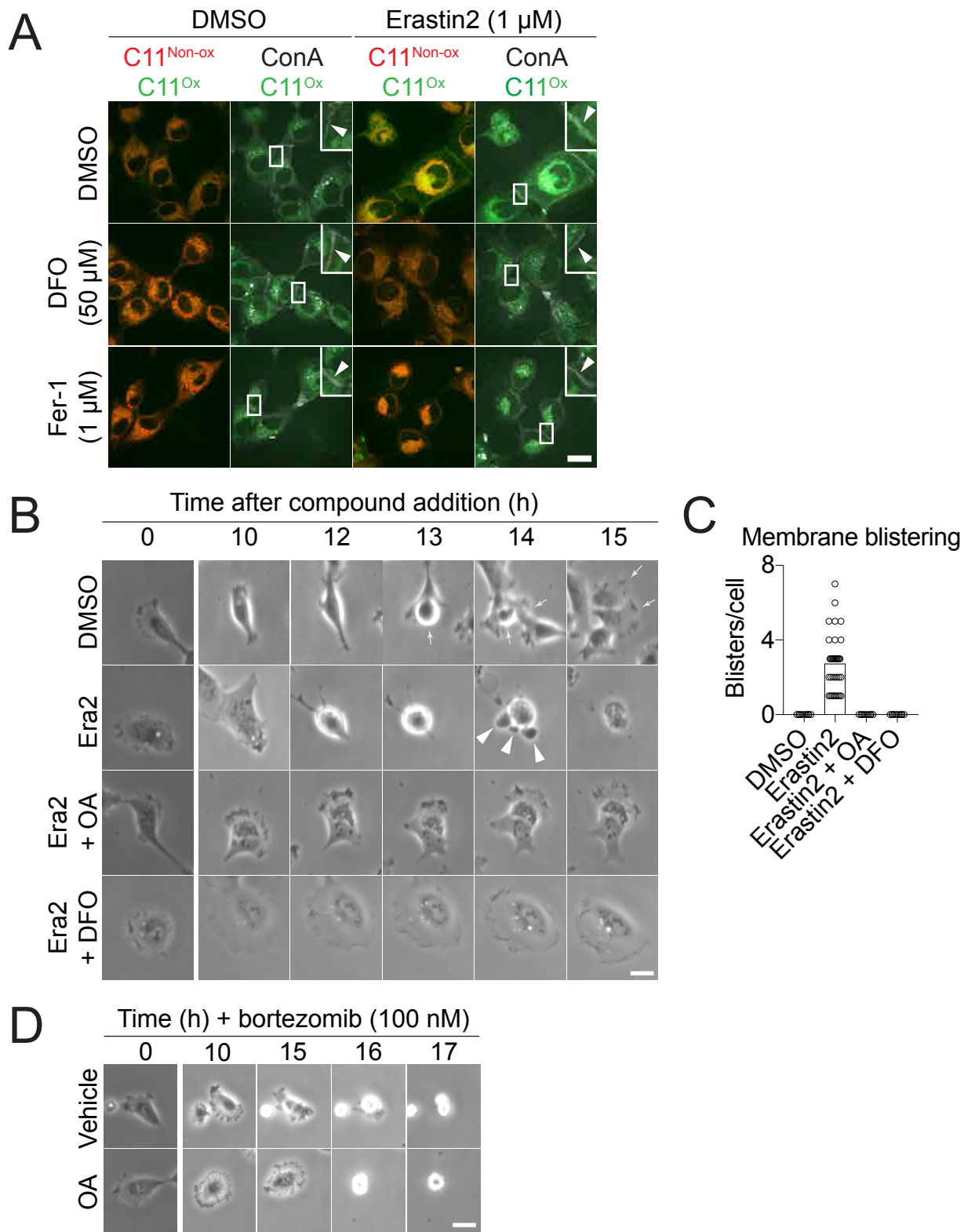


Figure S3, related to Figure 3. Membrane oxidation and morphological changes in ferroptotic cells. (A) C11 BODIPY 581/591 (C11) fluorescence imaging. HT-1080 cells were treated \pm erastin2 \pm deferoxamine (DFO) or ferrostatin-1 (Fer-1) for 10 h, then labeled with C11 (5 μ M) and assayed for oxidized (C11^{Ox}, green fluorescence) and non-oxidized (C11^{Non-ox}, red fluorescence) C11. Concanavalin A, Alexa Fluor 350 (ConA) (25 μ g/mL) was used to label the plasma membrane. The white arrowhead in the inset indicates C11^{Ox} and/or ConA labeling. The experiment was performed for two (Fer-1-treated samples) or four (DMSO- and DFO-treated) times and results from one experiment are shown. Scale bar = 20 μ m. (B) Representative images of HT-1080 cells treated over time treated with DMSO, erastin2 (Era2, 1 μ M) \pm OA (500 μ M) or + DFO (50 μ M). Erastin2-induced membrane blisters are indicated by arrowheads. In the DMSO-treated condition, arrows indicate a normal cell undergoing cell division. (C) Quantification of membrane blisters from cells in (B) (n = 10-35 cells / condition). (D) Representative images of HT-1080 cells treated with bortezomib \pm OA (500 μ M). In (B,D) the scale bar = 20 μ m.

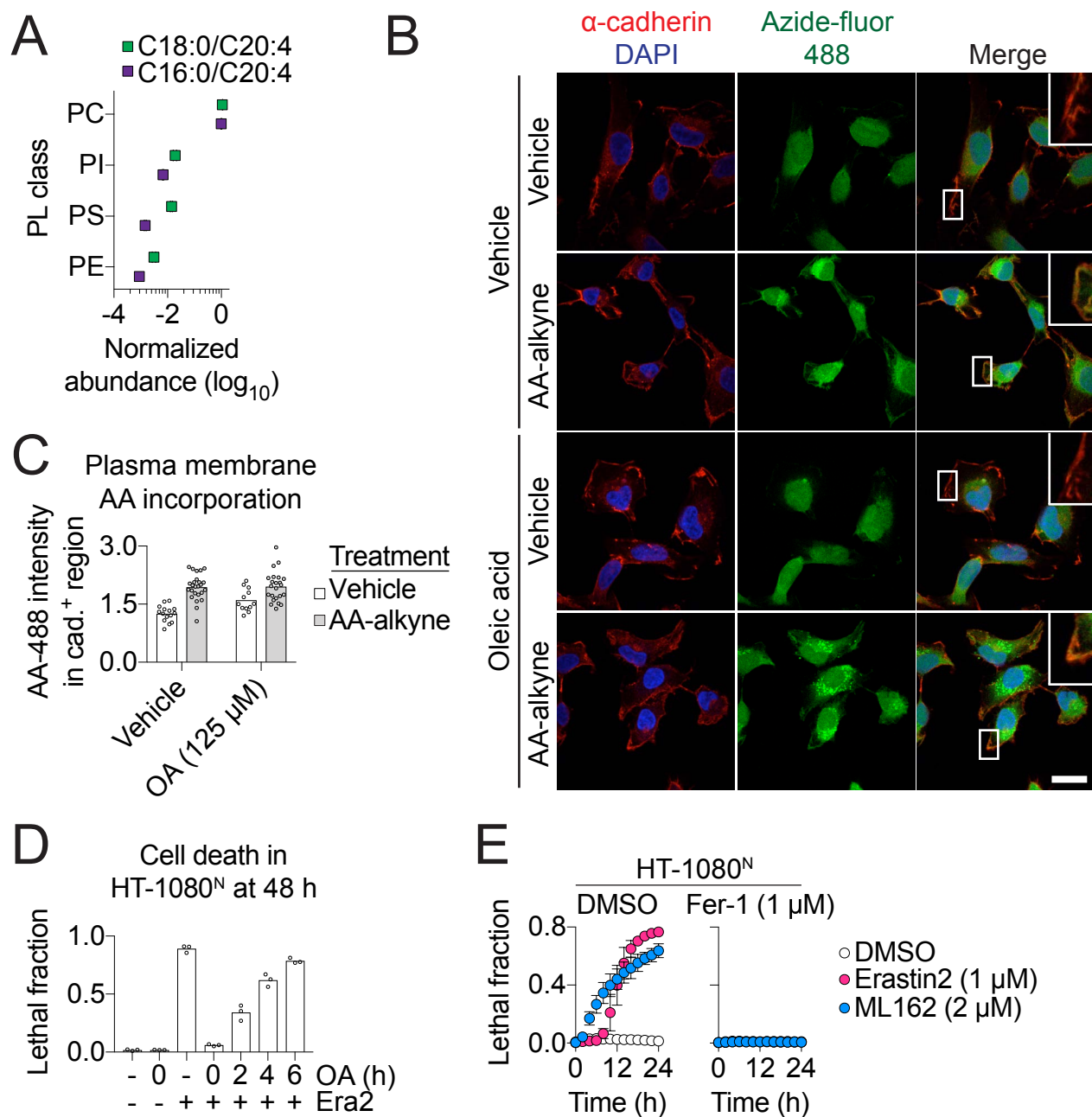


Figure S4, related to Figure 4. Modulation of phospholipid composition by MUFAs. (A) Relative abundance of C18:0/C20:4 and C16:0/C20:4 phospholipids (PLs) in HT-1080 cells treated under control conditions (DMSO/EtOH, 11 h). Data was obtained using single reaction monitoring liquid chromatography mass spectrometry. All values were normalized to C16:0/C20:4-PC, which was set at an arbitrary value of 1. Data are mean \pm SD from five independent biological replicates. (B) Visualization of arachidonic acid (AA) localization. HT-1080 cells were incubated with arachidonic acid-alkyne (AA-alkyne, 20 μ M) or vehicle control (ethanol, EtOH), and with either oleic acid (conjugated to bovine serum albumin [BSA], 125 μ M) or vehicle (BSA alone) for 2 h, then chased in regular medium for 2 h. AA-alkyne localization was visualized using copper-catalyzed click chemistry to azide-fluor 488, to yield AA-488. The plasma membrane is identified by cadherin immunofluorescence. Scale bar = 20 μ m. (C) Quantification of AA-488 fluorescence intensity within cadherin positive (cad.⁺) regions. Each data point represents a single image. Data are in arbitrary units (a.u. \times 10³). AA-488 imaging and quantification were performed on two independent biological replicates and results from one replicate are shown. (D) Effect of the timing of OA (125 μ M) addition on erastin2 (Era2, 1 μ M)-induced cell death. OA was added alone or at the same time as erastin2 (0), or 2, 4 or 6 h after the addition of erastin2. Each data point is from an independent biological replicate (n = 3). (E) Cell death over time. Data are the mean \pm SD from three independent biological replicates.

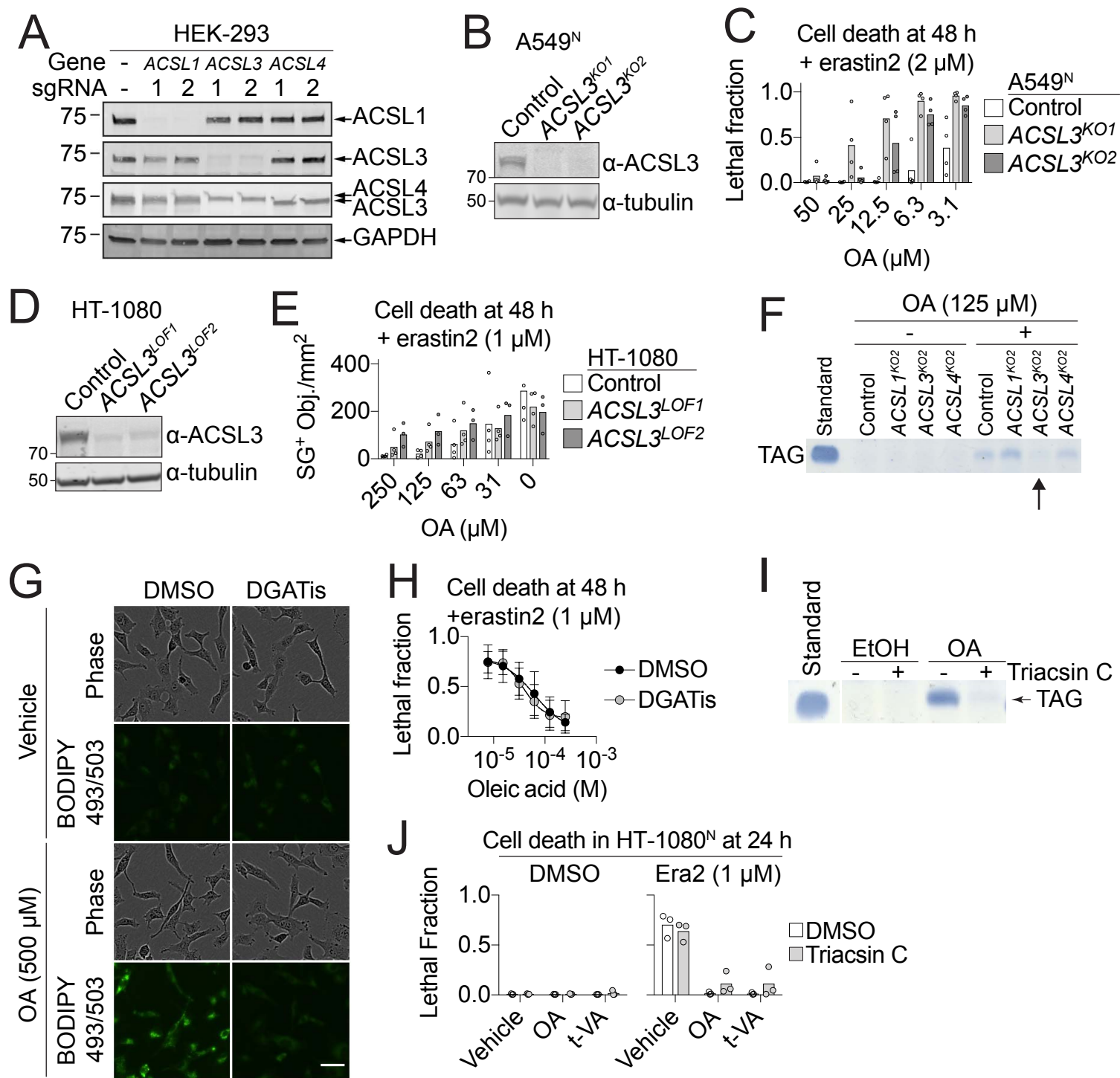


Figure S5, related to Figure 5. ACSL3 promotes OA-induced protection from ferroptosis. (A) Western blot of HEK-293 CRISPR/Cas9 control and knockout cell lines. The independent sgRNA 1 and 2 sequences for each gene are listed in the STARS Methods. The anti-ACSL4 antibody also recognizes ACSL3. (B) Western blots for A549^N Control and *ACSL3* gene-disrupted (KO) cell lines. (C) Cell death in A549^N Control and *ACSL3*^{KO1/2} cells treated as indicated. (D) Western blots for HT-1080 Control and *ACSL3* gene-disrupted cell lines. HT-1080 *ACSL3*^{LOF1} has mutations in both strands of the DNA at the *ACSL3* locus, and HT-1080 *ACSL3*^{LOF2} has a 6 bp deletion. As both cell lines may retain a small amount of ACSL3 protein as visualized by Western blotting, they are referred to as loss of function (LOF) rather than KO. (E) Cell death in HT-1080 Control and *ACSL3*^{LOF1/2} cells treated as indicated. (F) Neutral lipid (i.e. triacylglycerol, TAG) accumulation detected by thin layer chromatography in HEK-293 Control and ACSL knockout cell lines treated ± OA. (G) Neutral lipid detection using BODIPY 493/503 in HT-1080 cells treated ± oleic acid (OA, 500 μM) ± DGAT inhibitors (DGATis) for 6 h. DGATis: T863, 20 μM; PF-06424439, 10 μM. Scale bar = 50 μm. The experiment was performed on two independent biological replicates and results from one replicate are shown. (H) Cell death of HT-1080^N cells in response to OA ± DGATi treatment. DGATi concentrations are the same as in G. Data are mean ± SD from three biological replicates. (I) Thin layer chromatography of TAGs from HT-1080 cells treated for 6 h ± triacsin C (10 μM) ± OA (500 μM). Note: these extracts were run on the same TLC plate presented in Figure 5G and therefore the TAG standard presented here is the same as in Figure 5G. In (C,E) each data point is from an independent biological replicate.

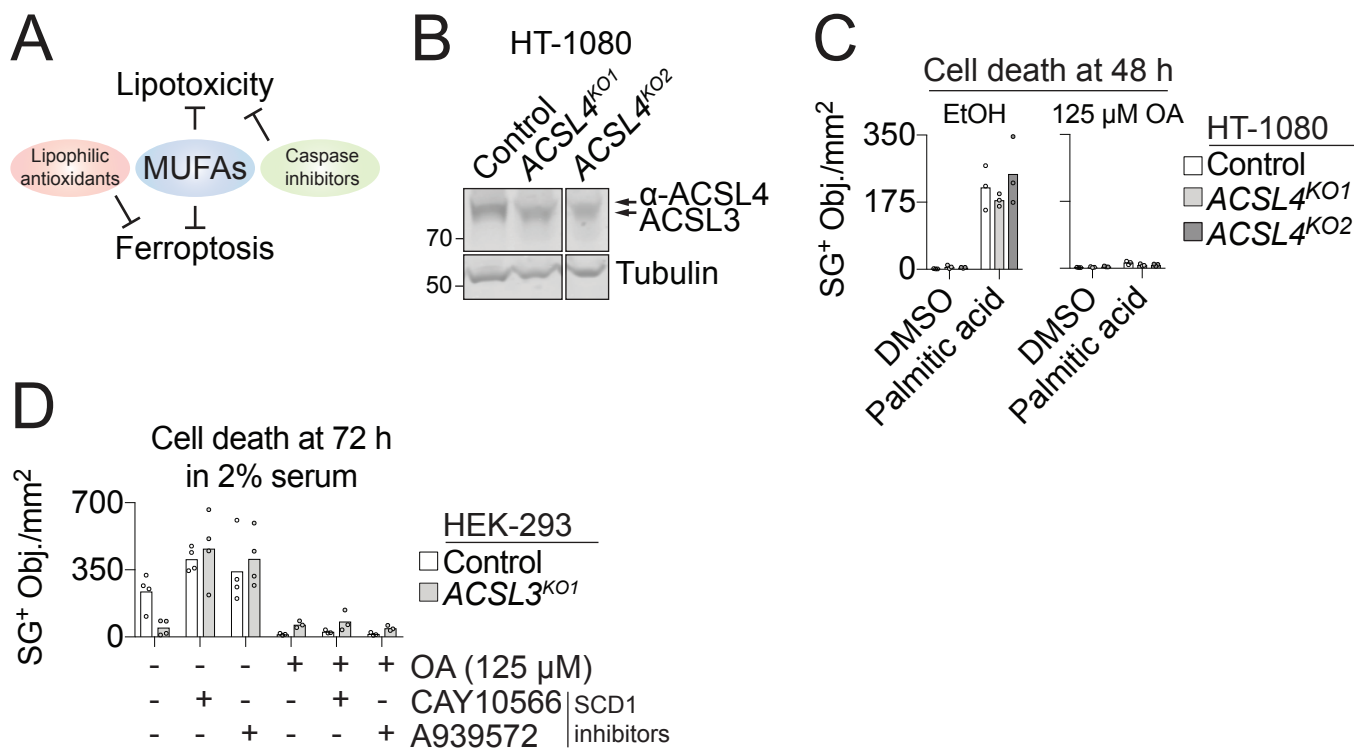


Figure S6, related to Figure 6. Lipotoxicity and ferroptosis are distinct. (A) Summary model of MUFA and inhibitor actions on lipotoxicity versus ferroptosis. (B) Western blot of HT-1080 CRISPR/Cas9 Control and *ACSL4* gene-disrupted (KO) cell lines. All three samples were run on the same gel but there were non-relevant samples run in between *ACSL4*^{KO1} and *ACSL4*^{KO2}, as indicated by the gap between the two samples. The anti-ACSL4 antibody also recognizes ACSL3 (see also Figure S5A). *ACSL4*^{KO1} and *ACSL4*^{KO2} were sequenced and verified to be genetic knockouts (see STARS Methods). (C) Cell death (SYTOX Green object counts (SG⁺Obj.) /mm²) in HT-1080 Control and *ACSL4*^{KO1/2} cell lines treated ± oleic acid (OA) ± palmitic acid (200 µM). (D) Cell death in HEK-293 Control and *ACSL3*^{KO1} cells treated as indicated. Each data point in (C,D) represents an independent biological replicate.

Table S1, related to Figures 2 and 5. Oligonucleotides used in this study.

OLIGO NAME and SEQUENCE	SOURCE	Identifier
<i>CHAC1</i> Forward 5'-GAACCCTGGTTACCTGGGC-3'	This paper	N/A
<i>CHAC1</i> Reverse 5'- CGCAGCAAGTATTCAAGTTGT-3'	This paper	N/A
<i>ACTB</i> Forward 5'-CATGTACGTTGCTATCCAGGC-3'	This paper	N/A
<i>ACTB</i> Reverse 5'- CTCCTTAATGTACGCACGAT-3'	This paper	N/A
<i>ACSL1</i> sg1 Forward 5'-CACCGACTTGACAGCGACGAGCCCT-3'	This paper	N/A
<i>ACSL1</i> sg1 Reverse 5'-AAACAGGGCTCGTCGCTGTCAAGTC-3'	This paper	N/A
<i>ACSL1</i> sg2 Forward 5'-CACCGCTCGTCGCTGTCAAGTAGTG-3'	This paper	N/A
<i>ACSL1</i> sg2 Reverse 5'-AAACCACTACTTGACAGCGACGAGC-3'	This paper	N/A
<i>ACSL3</i> sg1 Forward 5'-CACCGCGAGTGGATGATAGCTGCAC-3'	This paper	N/A
<i>ACSL3</i> sg1 Reverse 5'-AAACGTGCAGCTATCATCCACTCGC-3'	This paper	N/A
<i>ACSL3</i> sg2 Forward 5'-CACCGAGCTATCATCCACTCGGCC-3'	This paper	N/A
<i>ACSL3</i> sg2 Reverse 5'-AAACGGGCCGAGTGGATGATAGCTC-3'	This paper	N/A
<i>ACSL4</i> sg1 Forward 5'-CACCGTGCAATCATCCATTCGGCCC-3'	This paper	N/A
<i>ACSL4</i> sg1 Reverse 5'-AAACGGGCCGAATGGATGATTGCAC-3'	This paper	N/A
<i>ACSL4</i> sg2 Forward 5'-CACCGGTAGTGGACTCACTGCACT-3'	This paper	N/A
<i>ACSL4</i> sg2 Reverse 5'-AAACAGTGCAGTGAGTCCACTACC-3'	This paper	N/A
<i>ACSL3</i> amplicon Forward 5'-TGGCAATTCAAGTTCAGCAA-3'	This paper	N/A
<i>ACSL3</i> amplicon Reverse 5'-GTTCAAGCCTCACTGCAACA-3'	This paper	N/A
<i>ACSL3</i> sequencing primer 5'-ACAGAGTTCTCCACTAACTGG-3'	This paper	N/A
<i>ACSL4</i> amplicon Forward 5'-ACCCCCAACTCCAACCTTT-3'	This paper	N/A
<i>ACSL4</i> amplicon Reverse 5'-GGGACCAGGGAAATCCTAAG-3'	This paper	N/A
<i>ACSL4</i> sequencing primer 5'-TAAAATGGCTAAACAACACC-3'	This paper	N/A